

# Epitaxial Crystallization of Isotactic Poly(Methyl Methacrylate) on Highly Oriented Polyethylene

Jing Liu,<sup>†</sup> Jijun Wang,<sup>†</sup> Huihui Li,<sup>†</sup> Deyan Shen,<sup>†</sup> Jianming Zhang,<sup>‡</sup> Yukihiro Ozaki,<sup>\*,‡</sup> and Shouke Yan<sup>\*,†</sup>

State Key Laboratory of Polymer Physics and Chemistry, Institute of Chemistry, The Chinese Academy of Sciences, Beijing 100080, P. R. China, and Department of Chemistry, School of Science and Technology, Kwansei-Gakuin University, Gakuen, Sanda 669-1337, Japan

Received: June 22, 2005; In Final Form: November 14, 2005

The annealing behavior of amorphous i-PMMA thin films on highly oriented HDPE substrates was studied by transmission infrared spectroscopy and electron diffraction. The i-PMMA thin film on highly oriented HDPE exhibits a much faster crystallization rate than usual, providing not only a good method for the preparation of crystalline i-PMMA thin and ultrathin film, but also the convenience to observe the crystallization process by infrared spectroscopy in situ. The overall crystallization kinetics of the i-PMMA thin film on the highly oriented HDPE layer was also explored in this work, and an Avrami exponent of about 2 was obtained. The accelerated crystallization behavior indicates a special interaction between HDPE and i-PMMA, which favors the nucleation and crystallization of i-PMMA. This special interaction leads also to an oriented alignment of i-PMMA on the HDPE substrate with both polymer chains parallel, i.e., the occurrence of heteroepitaxy, which could be verified by the polarized infrared spectra and electron diffraction pattern. Electron diffraction analysis further demonstrated that the contact planes of this epitaxial system are (100) lattice planes of both polymers. This can be explained in terms of a two-dimensional lattice matching.

## Introduction

Crystallization of polymers in thin and ultrathin films may exhibit different character from that in bulk. As is well-known, when the thickness of the polymer films is sufficiently small, the growth of a spherulite in the direction vertical to the film plane is limited,<sup>1,2</sup> and with further decrease, more significant distinctions arise, such as retarded lamellar growth rate and low degree of crystallinity.<sup>3</sup> In extreme cases, for some particular polymers, the work to cultivate crystallinity in thin and ultrathin films becomes very difficult. For example, isotactic poly(methyl methacrylate)(i-PMMA), which is not only famous for its interesting double-stranded helix structure similar to bimolecular DNA in its crystal, but also notorious for its extremely slow crystallization rate, is one of this kind of polymers.<sup>4–7</sup>

Since the first report of stereoregular poly(methyl methacrylate)s in 1958 by Fox et al.,<sup>8</sup> the crystalline structure<sup>9–11</sup> and morphology<sup>5,12</sup> and other particular properties have been studied. Isotactic and syndiotactic isomers (i-PMMA and s-PMMA) can form not only ordered self-associated structures, respectively, but also exhibit stereocomplex structure under some preparative conditions.<sup>13–15</sup> Recently, the self-assembly of stereoregular PMMA,<sup>16,17</sup> template polymerization,<sup>18</sup> synthesis of PMMA-silica,<sup>19</sup> and interface behavior,<sup>20</sup> which are all related to stereocomplexation, have come under study.

The structure of i-PMMA crystals has been disputed since the first reports,<sup>8–11</sup> and was primarily determined by Kusanagi et al.<sup>9</sup> in 1994. i-PMMA exhibits an orthorhombic cell with  $a$

$= 4.196$  nm,  $b = 2.434$  nm, and  $c = 1.05$  nm. The packing mode of 10/1 double-stranded helices is eight right- and left-handed molecules in one unit cell. In the past several years, the crystalline structure<sup>9–11</sup> and morphology<sup>12</sup> of uniaxially oriented i-PMMA crystals, achieved by stretching and annealing, have been studied. It was reported that, for amorphous i-PMMA ultrathin films with a thickness of hundreds of angstroms, crystallization did not take place significantly even after 1 month of annealing at 120 °C,<sup>21</sup> which is the optimum crystallization temperature. A similar phenomenon was observed in our experiments.

In the early nineties of the last century, Schouten et al.<sup>6</sup> reported a fast crystallization process for i-PMMA under a crystalline i-PMMA Langmuir–Blodgett film; this phenomenon was attributed to homoepitaxy. A question arises whether heteroepitaxy, which is one branch of the self-assembly field,<sup>22,23</sup> can also induce a similar fast crystallization process of i-PMMA in thin and ultrathin films. In this paper, the unique crystallization behavior of i-PMMA thin films on highly oriented high-density polyethylene (HDPE) substrates is presented.

## Experimental Section

**2.1. Material and Preparation Procedures.** Isotactic PMMA material was purchased from Polymer Science, Inc., Canada. The tacticity of PMMA is 97% isotactic. The molecule weight is 4.35 kg/mol with a polydispersity of 1.13. The high-density polyethylene (HDPE) used in this work is Lupolen 6021DX from BASF AG Ludwigshafen, Germany.

Uniaxially oriented thin HDPE films were prepared according to a melt–draw technique introduced by Petermann and Gohil.<sup>24</sup> According to this method, a small amount of a 0.5 wt % solution of the HDPE in xylene was poured and uniformly spread on a

\* To whom all correspondence should be addressed. E-mail: skyan@iccas.ac.cn. Telephone: 0086–10–82618476. Fax: 0086–10–82618476.

<sup>†</sup> State Key Laboratory of Polymer Physics and Chemistry, Institute of Chemistry.

<sup>‡</sup> Department of Chemistry, School of Science and Technology.

preheated glass plate, where the solvent was allowed to evaporate at the preparation temperature. After evaporation of the solvent, the HDPE thin molten layer was then drawn up by a motor-driven cylinder with a drawing speed of about 2 cm/s. The thickness of the obtained thin films ranges from 30 to 50 nm. The HDPE thin films were first annealed at 120 °C for 4 h under the protection of nitrogen, before further sample preparation, to eliminate any spectra change of HDPE during the annealing of i-PMMA/HDPE double layers.

Samples for transmission infrared measurements were prepared by casting a 0.5 wt % solution of i-PMMA in chloroform on HDPE thin films supported on KBr substrates. The thickness of the films for transmission IR measurements was calculated from the amount of cast solution to be 0.5–1  $\mu\text{m}$ .

Samples for transmission electron microscopy (TEM) observation were prepared by casting a 0.1 wt % solution of i-PMMA on the HDPE film surface. The thickness of the i-PMMA films for TEM was measured to be 100–150 nm by AFM with the scratch method.<sup>25</sup> All prepared samples were annealed on a hot stage at 120 °C for a predetermined period of time.

**2.2. Fourier Transform IR Spectroscopy.** IR spectra were recorded on a Bruker EQUINOX 55 spectrometer and processed by the Bruker OPUS program. For in situ TIR spectra acquisition, the specimen was set in a Bruker P/N 21525 series variable temperature cell, which was placed in the sample compartment equipped with a DTGS detector. The measurements were obtained by using an average of 32 scans and a resolution of 4  $\text{cm}^{-1}$ , only for in situ IR observation, the background was chosen as the HDPE thin film before the deposition of i-PMMA to decrease the effect of the HDPE layer in the analysis of the spectra.

**2.3. Transmission Electron Microscopy.** For TEM observation, a JEM-100 CXII transmission electron microscopy, operated at 100 kV, was used.

### 3. Results and Discussion

**3.1. Crystallization of i-PMMA on Highly Oriented HDPE Substrate during Annealing.** The morphology development of i-PMMA in films was always followed by using phase-contrast microscopy. The temperature for the maximum growth rate was reported to be 120 °C, at which the growth rate of i-PMMA crystals was estimated to be 1/300 of that of isotactic polystyrene.<sup>5</sup> Consequently, the temperature of 120 °C was chosen as the annealing temperature also in our experiments. After 14 days' annealing at 120 °C, Schneider et al.<sup>26</sup> prepared crystalline i-PMMA films. Differences in the infrared spectra between crystalline and amorphous samples of i-PMMA were studied. The bands at 1339, 1295, and 882  $\text{cm}^{-1}$  were assigned to the characteristic bands of the crystalline phase, while the bands at 1047 and 938  $\text{cm}^{-1}$  were attributed to its amorphous phase. In the later researches, the band at 1295  $\text{cm}^{-1}$ , which has not been found in amorphous i-PMMA, becomes the most frequently used characteristic band to judge the occurrence of crystallization.<sup>6,21</sup> Figure 1 shows the IR spectra of i-PMMA on highly oriented HDPE thin films before and after annealing. From Figure 1, the absence of the 1295  $\text{cm}^{-1}$  band in the IR spectrum of the as-prepared sample indicates that the solution-cast i-PMMA films on highly oriented HDPE substrate are amorphous. This has been further confirmed by electron diffraction (figure not shown). This result is similar to those for solution-cast i-PMMA films on other substrates and indicates that the HDPE substrate exhibits no evident influence on the solvent evaporation process of i-PMMA. After 48 h annealing

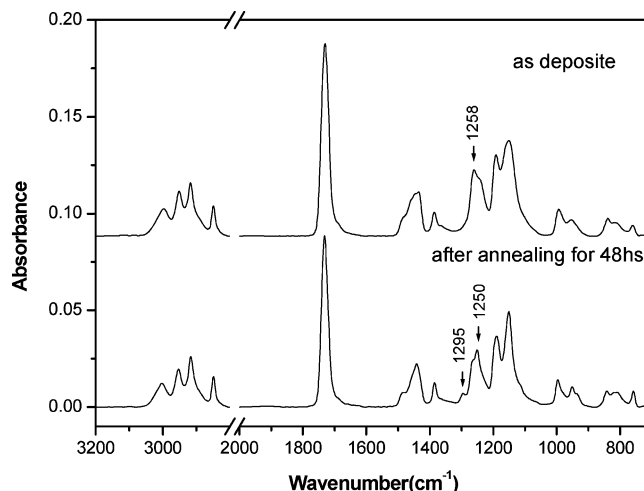


**Figure 1.** IR spectra of an i-PMMA/HDPE double-layered film before and after annealing. The annealing was held at 120 °C for 48 h.

at 120 °C, the characteristic crystalline band of i-PMMA at 1295  $\text{cm}^{-1}$  appears. There are also shape changes of the bands related to the ester group in the range of 1300–1050  $\text{cm}^{-1}$ . These changes undoubtedly verify the occurrence of i-PMMA crystallization. This is different from the annealing behavior of pure i-PMMA films (without HDPE support) with the same thickness, where no visible absorbance at 1295  $\text{cm}^{-1}$  can be observed, even after 72 h annealing at the same temperature. This implies that the existence of highly oriented HDPE layers has promoted the crystallization of i-PMMA thin films greatly.

The extremely slow crystallization process of i-PMMA makes it difficult for an in situ study on its crystallization process. Therefore, the structure change during crystallization has not been known definitely. The elevated crystallization rate of i-PMMA on HDPE substrate enables us to follow its crystallization process in real time. Figure 2a shows the time-resolved IR spectrum of i-PMMA during the isothermal crystallization process at 120 °C. From Figure 2a, some changes in the IR spectrum can be identified, but the interpretation is not quite clear because of the overlap of the absorption bands. For clarity, Figure 2b shows the time-resolved IR spectrum with the initial spectrum being subtracted, i.e., the difference spectrum. Now one can see in more detail the changes in the spectrum during the crystallization process. Because the 1295  $\text{cm}^{-1}$  band is the well-known crystallization-sensitive band of i-PMMA,<sup>11,21,26–27</sup> the intensity increase of the band at 1295  $\text{cm}^{-1}$  indicates that the crystallization of i-PMMA on the HDPE layer proceeds during the annealing.

Moreover, it can be found that the intensity of the band at 756  $\text{cm}^{-1}$ , which is assigned to skeletal stretching, coupled with rocking vibration of  $\text{CH}_2$ , increases with the proceed of crystallization. This absorption reflects the conformational change of the backbone directly. Another pair of bands at 967 and 950  $\text{cm}^{-1}$  also exhibits obvious variation during the crystallization. Dybal et al.<sup>28</sup> have assigned the 950  $\text{cm}^{-1}$  band to the energetically more-favored backbone conformation of i-PMMA, while the band at 967  $\text{cm}^{-1}$  has been assigned to the less-favored conformation. This is in good accordance with our results that the absorbance at 950  $\text{cm}^{-1}$  increases, while the 967  $\text{cm}^{-1}$  band decreases during the crystallization process. At the same time, the intensity of the bands related to the ester group, ranging from 1300 to 1000  $\text{cm}^{-1}$ , apparently also varies. In early studies on stereoregular PMMA, the conformation sensitive bands at 1300–1050  $\text{cm}^{-1}$  have revealed a strong temperature dependence and were used in the conformational energy

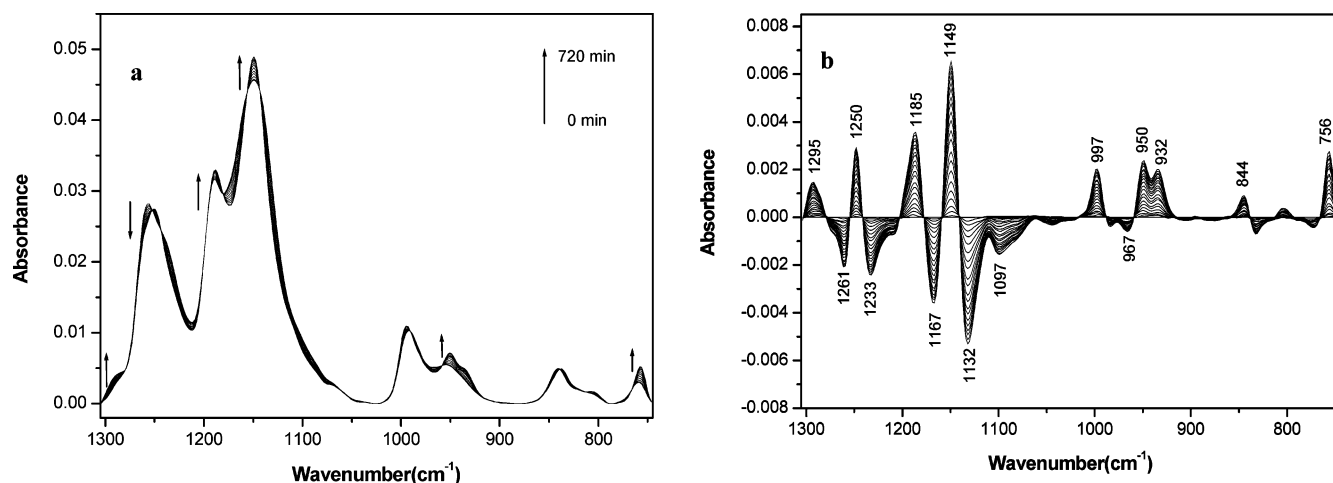


**Figure 2.** Time-dependent IR spectra of an i-PMMA/HDPE double-layered film in the range of 1305–745  $\text{cm}^{-1}$ , collected during the annealing process (a), and the corresponding difference spectra (b). The spectra were recorded from 0 to 720 min with 30 min intervals.

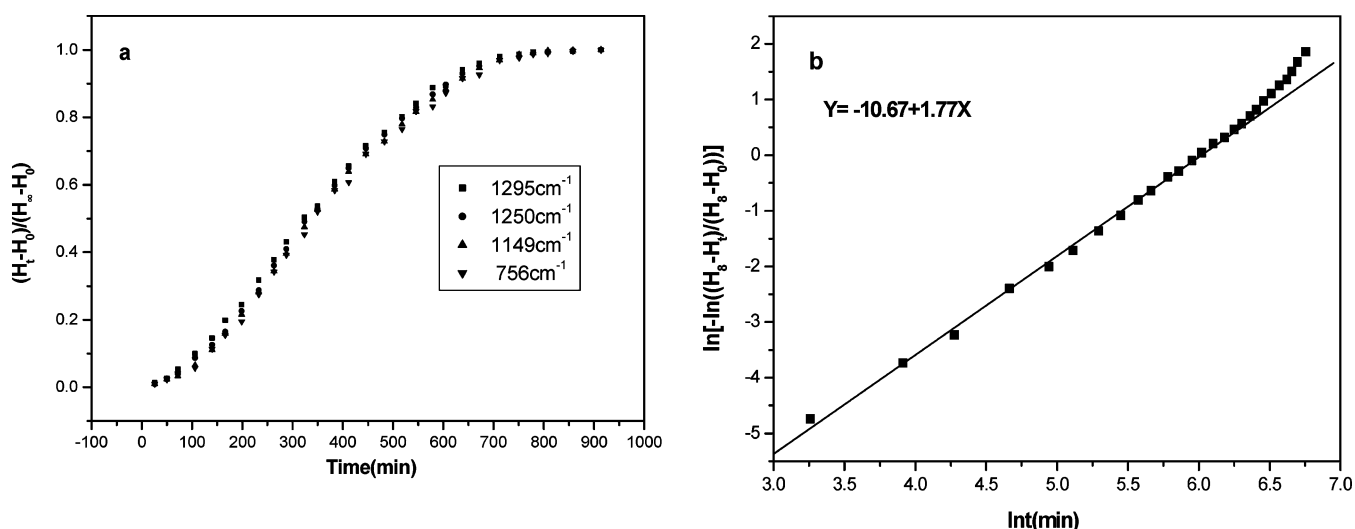


**Figure 3.** Normalized peak height of the crystallization sensitive bands at 1295, 1250, 1149, and 760  $\text{cm}^{-1}$  as the function of annealing time (a) and a generated Avrami plot from the data of band at 1250  $\text{cm}^{-1}$  (b).  $H_t$ ,  $H_0$ , and  $H_\infty$  present the intensity of the band in the IR spectra at time  $t$ , at the beginning of annealing and after 914 min of annealing at 120  $^{\circ}\text{C}$ .

determination.<sup>28–30</sup> As shown in Figure 2b, a new absorption band at 1250  $\text{cm}^{-1}$  appears, which has not been found in amorphous i-PMMA.<sup>29</sup> Grohens et al.<sup>31</sup> have observed a gradual shift of the band at 1258  $\text{cm}^{-1}$  to 1250  $\text{cm}^{-1}$  during their study on PMMA with different tacticity. They attributed this shift to the change in conformation of backbone and the side-group interaction. It is stated that, with increasing isotactic content, stronger side-group interaction and more TT states in the backbone exist, and these cause the band shifts to lower wavenumbers. Considering the all-trans backbone chain conformation of i-PMMA in the crystalline state,<sup>32</sup> the appearance of 1250  $\text{cm}^{-1}$  may correspond to the emergence of long TT sequences during the transition from amorphous to crystalline states in the i-PMMA layer. Therefore, the intensity change of this crystallization-sensitive band with annealing time was used to study the crystallization kinetics of i-PMMA on HDPE substrate. For comparison, the intensity changes of the 1295, 1149, and 760  $\text{cm}^{-1}$  bands are also followed.

Figure 3a plots the normalized peak height of the crystallization sensitive bands at 1295, 1250, 1149, and 760  $\text{cm}^{-1}$  as a function of crystallization time at 120  $^{\circ}\text{C}$ . They show similar typical “S” shape. With the data in Figure 3a, the Avrami plots for the epitaxial crystallization process of i-PMMA on the highly oriented HDPE layer are constructed. The calculated Avrami

exponents of these bands range from 1.73 to 1.80, which are well fit in the experimental error range. As an example, Figure 3b shows the Avrami plot of the 1295  $\text{cm}^{-1}$  band. The Avrami exponent  $n$  of it is calculated to be 1.77. As is well-known, the Avrami exponent  $n$  is characteristic of the nucleation type and the crystal growth geometry. A value of 3–4 is usually adopted for polymer bulk crystallization. It may drop to 2 for the growth in two dimensions of thin film. It was reported that crystallization in the great constrained circumstance, such as the crystallization in ultrathin films and for block copolymers with a glassy matrix and minority crystallizable block,<sup>33,34</sup> results in further decrease in the Avrami exponent.<sup>33–35</sup> A value of  $n = 1$  has been reported for the strain-induced crystallization of polymers,<sup>36</sup> where alignment of molecular chains induces massive nucleation and the growth is one-dimensional. Brinkhuis and Schouten<sup>6</sup> have reported the  $n = 1$  kinetics of the homoepitaxial crystallization of the amorphous i-PMMA thin film, with a thickness of 3  $\mu\text{m}$  induced by crystalline i-PMMA LB ultrathin film. They attributed the Avrami exponent to instantaneous nucleation followed by one-dimensional growth, which is similar to the case of strain-induced crystallization. Our experimental result may imply a two-dimensional crystal growth process of i-PMMA on the HDPE. This is different from the self-induced homoepitaxy.

**TABLE 1: Assignment of Relevant IR Absorption Bands of i-PMMA<sup>11,21,26–27</sup> and HDPE<sup>37a</sup>**

wavenumber (cm <sup>-1</sup> ) crystalline/amorphous	dichroism	assignment	
2997		$\nu_a(\text{CH}_3\text{--O}) + \nu_a(\text{CH}_2)$	i-PMMA
2950	⊥	$\nu_s(\text{CH}_3\text{--O}) + \nu_a(\alpha\text{--CH}_2) + \nu_s(\alpha\text{--CH}_2) + \nu_s(\text{CH}_2)$	i-PMMA
2918	⊥	$\nu_a(\text{CH}_2)$	HDPE
2850	⊥	$\nu_s(\text{CH}_2)$	HDPE
1732	⊥	$\nu(\text{C=O})$	i-PMMA
1296/- - -	⊥	characteristic for crystalline	i-PMMA
1263		$\nu$	i-PMMA
1250/1240	⊥		i-PMMA
1149	⊥	skeletal stretching coupled with C–H deformation vibration	i-PMMA
1192	⊥	$\nu_a(\text{C--O--C})$	i-PMMA
950		$\gamma(\alpha\text{--CH}_3)$	i-PMMA
760		skeletal $\nu(\text{C--C})$ coupled with $\gamma(\text{CH}_2)$	i-PMMA

<sup>a</sup> The following abbreviations have been used:  $\nu_a$  = asymmetric stretching,  $\nu_s$  = symmetric stretching, and  $\gamma$  = rocking.

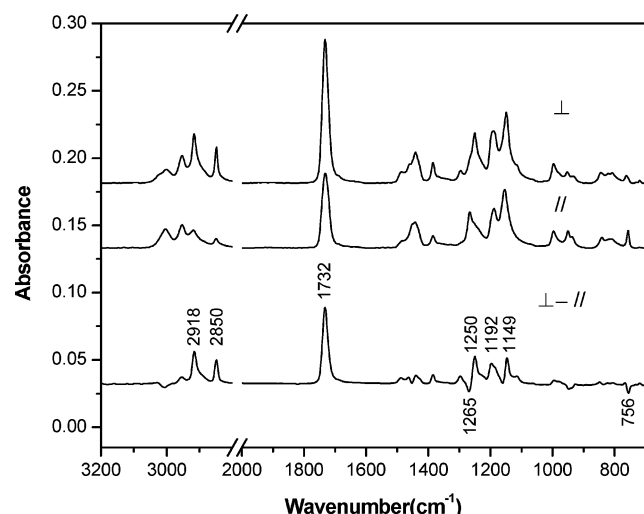
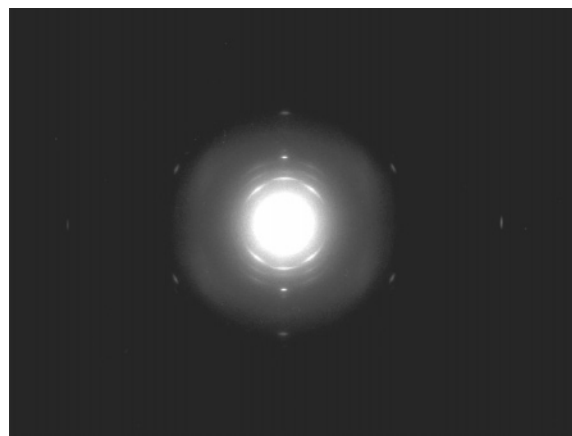


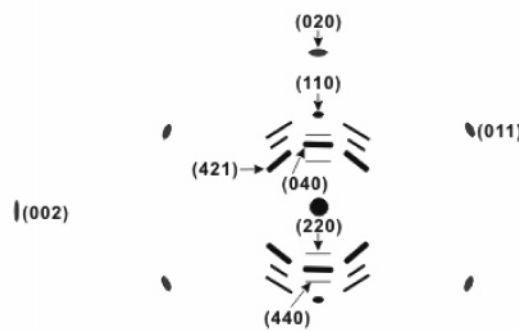
**Figure 4.** Polarized IR spectra of the i-PMMA/HDPE double layers after 48 h isothermal crystallization at 120 °C. (⊥) means the electron vector perpendicular to the draw direction of HDPE; (||) means the electron vector parallel to the draw direction of HDPE, and (⊥ - ||) indicates the difference spectra.

**3.2. Orientation of i-PMMA on the Highly Oriented HDPE Substrate.** From the above discussion, it is known that HDPE exhibits strong nucleation ability toward i-PMMA, which promotes the crystallization of i-PMMA tremendously. Strong heterogeneous nucleation ability may also induce an oriented

crystallization of a polymer, i.e., heteroepitaxy. To check the orientation of i-PMMA on highly oriented HDPE substrate, polarized infrared spectroscopy was used. Figure 4 shows the polarized infrared spectrum of the i-PMMA/HDPE double layers annealed for 48 h at 120 °C. From Figure 4, differences between the IR spectra with the electron vector perpendicular “⊥” and parallel “||” to the drawing direction of the HDPE thin film during preparation can be recognized. This can be more clearly seen from the difference spectrum, i.e., a subtraction of IR spectrum with electron vector perpendicular from the IR spectrum with electron vector parallel (bottom part of Figure 4). In the difference spectrum, the vibrations exhibiting perpendicular transition moment with respect to the drawing direction should appear as positive peaks. It is clear that the bands at 2918 and 2850 cm<sup>-1</sup>, assigned to the stretching vibration of CH<sub>2</sub> groups of HDPE, and which exhibit perpendicular transition moment with respect to the main chains of HDPE,<sup>37</sup> reveal themselves as positive peaks in difference spectra. This means that the main chain of HDPE is parallel to the drawing direction, which is in good agreement with the electron diffraction result.<sup>38,39</sup> For i-PMMA, as summarized in Table 1, there are several perpendicular bands of i-PMMA: the bands at 1732 cm<sup>-1</sup>, attributed to the stretching vibration of C=O; bands at 1250 and 1192 cm<sup>-1</sup>, related to the ester group. The band at 1149 cm<sup>-1</sup>, which is associated with the mixed vibrations of the skeletal stretching, CH<sub>2</sub> twisting, and other internal carbon–hydrogen deformation vibrations, is also perpendicularly polar-



(a)



(b)

**Figure 5.** (a) Electron diffraction pattern and (b) its corresponding sketch with main reflections being indexed of i-PMMA/HDPE double layers annealed at 120 °C for 72 h. In the sketch, the solid ellipses represent the diffraction spots of oriented HDPE substrate crystals, while the lines represent the reflections of the i-PMMA crystals.



ized.<sup>27</sup> Conversely, the band at 756 cm<sup>-1</sup>, which is assigned to the skeletal stretching vibration coupled with  $\gamma(\text{CH}_2)$  vibration, is parallel polarized.<sup>27</sup> The positive perpendicular bands and negative parallel bands displayed in the difference spectra clearly indicate that the main chains of i-PMMA in the double-layered thin films are aligned preferentially parallel to the chain direction of HDPE, indicating heteroepitaxy of i-PMMA on the HDPE substrate, with both molecular chains parallel. This is further confirmed by the electron diffraction result.

Figure 5a presents the electron diffraction (ED) pattern of the i-PMMA/HDPE double-layered thin films annealed at 120 °C for 72 h. A sketch of the electron diffraction pattern with the main reflections being indexed is reported in Figure 5b. In Figure 5a, except for the well-known HDPE reflections, all of the observed i-PMMA reflections are accounted for by the orthorhombic unit cell with axes  $a = 4.196$  nm,  $b = 2.434$  nm, and  $c = 1.05$  nm, as proposed by Kusanagi et al.<sup>9</sup> The appearance of well-defined reflection spots and arcs of both i-PMMA and HDPE on the electron diffraction pattern confirms that i-PMMA crystallizes epitaxially on the highly oriented HDPE substrate after 72 h annealing at 120 °C. The alignment of  $(hk0)$  for i-PMMA in the  $[hk0]$  direction of HDPE reflects a parallel orientation of i-PMMA and PE chains. This is in good agreement with the IR results. Several features of the ED pattern provide detailed information about the epitaxial crystallization of i-PMMA on the HDPE substrate. First of all, for the HDPE substrate, the tremendous intensity decrease of  $(110)$  reflections, the absence of  $(200)$  diffraction spots, and the appearance of strong  $(020)$  reflections suggests that the HDPE highly oriented thin films exhibit a double texture, with the crystallographic  $c$ - and  $b$ -axes oriented preferentially in the film plane.<sup>40</sup> On the other hand, the absence of  $(400)$  diffraction spots and the appearance of strong  $(040)$  i-PMMA diffraction spots on the meridian indicates that the  $(100)$  lattice plane is its exposed plane.<sup>41</sup> In other words, the  $(100)_{\text{PMMA}}$  lattice plane is in contact with the HDPE substrate. Therefore, the epitaxial relationship between i-PMMA and HDPE may be as follows:

$$\begin{aligned} &[001]_{\text{PE}} // [001]_{\text{i-PMMA}} \\ &(100)_{\text{PE}} // (100)_{\text{i-PMMA}} \end{aligned}$$

By keeping the orthorhombic cell of HDPE with axes  $a = 0.74$  nm,  $b = 0.493$  nm, and  $c = 0.2534$  nm in mind,<sup>42</sup> the observed epitaxy may be explained in terms of a two-dimensional lattice matching between the  $bc$  planes of both polymers. While a perfect matching can be found between the interplane distance of i-PMMA and five times the interplane distance of HDPE both in  $[010]$  directions with a mismatching of 1.3%, a mismatching of about 3.5% along the chain axes of both polymer is also well within the upper limit (10–15%) for the occurrence of polymer epitaxy.<sup>43</sup>

#### 4. Conclusions

The annealing behavior of i-PMMA thin film on highly oriented HDPE crystalline substrate was studied by IR spectroscopy and electron diffraction. The IR in-situ study shows that the crystallization rate of i-PMMA on a highly oriented HDPE substrate is increased tremendously. This indicates that HDPE exhibits strong nucleation ability toward i-PMMA. Polarized IR and electron diffraction results further demonstrated that the existence of special interaction between i-PMMA and HDPE results in an oriented alignment of i-PMMA on the HDPE substrate with both polymer chains parallel, i.e., the occurrence of heteroepitaxy. In this epitaxial system, the contact planes of

both HDPE and i-PMMA are the  $(100)$  lattice planes. This can be explained in terms of a two-dimensional lattice matching.

**Acknowledgment.** We thank Prof. J. M. Schultz for his useful discussion and English correction. The financial support of the Outstanding Youth Fund (no. 20425414) and the National Natural Science Foundation of China (nos. 20374056, 20304018, and 20423003) are also gratefully acknowledged.

#### References and Notes

- (1) Stein, R. S. *J. Polym. Sci.* **1962**, *56*, S9.
- (2) Billon, N.; Haudin, J. M. *Colloid Polym. Sci.* **1989**, *267*, 1064.
- (3) Schönherr, H.; Frank, C. W. *Macromolecules* **2003**, *36*, 1199.
- (4) Zhao, D.; Li, L.; Che, B.; Cao, Q.; Lu, Y.; Xue, Q. *Macromolecules* **2004**, *37*, 4744.
- (5) De Boer, A.; Alberda van Ekenstein, G. O. R.; Challa, G. *Polymer* **1975**, *16*, 930.
- (6) Brinkhuis, R. H. R.; Schouten, A. J. *Macromolecules* **1992**, *25*, 2717.
- (7) Mitchell, G. R.; Windle, A. H. *Colloid Polym. Sci.* **1982**, *260*, 754.
- (8) Fox, T. G.; Garret, B. S.; Goode, W. E.; Gratch, S.; Kincaid, J. F.; Spell, A.; Stroupe, J. D. *J. Am. Chem. Soc.* **1958**, *80*, 1768.
- (9) Kusanagi, H.; Chatani, Y.; Tadokoro, H. *Polymer* **1994**, *35*, 2028.
- (10) Špeváček, J.; Schneider, B.; Straka, J. *Macromolecules* **1990**, *23*, 3042.
- (11) Dybal, J.; Krimm, S. *Macromolecules* **1990**, *23*, 1301.
- (12) Klement, J. J.; Geil, P. H. *J. Macromol. Sci., B* **1972**, *6*, 31.
- (13) Špeváček, J.; Schneider, B. *Adv. Colloid. Interface Sci.* **1987**, *27*, 81.
- (14) Takashi, T.; Kojima, K.; Maegawa, T. *Polymer* **1999**, *40*, 3301.
- (15) Buyse, K.; Berghmans, H. *Macromolecules* **1998**, *31*, 9224.
- (16) Serizawa, T.; Hamada, K.-I.; Kitayama, T.; Fujimoto, N.; Hatada, K.; Akashi, M. *J. Am. Chem. Soc.* **2000**, *122*, 1891.
- (17) Serizawa, T.; Hamada, K.-I.; Kitayama, T.; Akashi, M. *Angew. Chem., Int. Ed.* **2003**, *42*, 1118.
- (18) Serizawa, T.; Hamada, K.-I.; Akashi, M. *Nature* **2004**, *429*, 52.
- (19) Kumar, A. A.; Adachi, K.; Chujo, Y. *J. Polym. Sci., Polym. Chem.* **2004**, *42*, 785.
- (20) Wang, J.; Shen, D.; Yan, S.; *Macromolecules* **2004**, *37*, 8171.
- (21) Brinkhuis, R. H. R.; Schouten, A. J. *Macromolecules* **1991**, *24*, 1496.
- (22) Whitesides, G. M.; Grzybowski, B. *Science* **2002**, *295*, 2418.
- (23) Yanagi, H.; Yamane, K.; Fukushima, M.; Hayakawa, T. *J. Phys. Chem. B* **2003**, *107*, 12201.
- (24) Petermann, J.; Gohil, R. M. *J. Mater. Sci.* **1979**, *14*, 2260.
- (25) Zhang Y.; Zhang J.; Lu Y.; Duan Y.; Yan S.; Shen D. *Macromolecules* **2004**, *37*, 2532.
- (26) Schneider, B.; Štokr, J.; Špeváček, J.; Baldrian, J. *Macromol. Chem.* **1987**, *188*, 2705.
- (27) Nagai, H. *J. Appl. Polym. Sci.* **1963**, *7*, 1697.
- (28) Dybal, J.; Štokr, J.; Schneider, B. *Polymer* **1983**, *24*, 971.
- (29) Tretinnikov, O. N.; Ohta, K. *Macromolecules* **2002**, *35*, 7343.
- (30) O'Reilly, J. M.; Mosher, R. A. *Macromolecules* **1983**, *22*, 175.
- (31) Grohens, Y.; Prud'homme, R. E.; Schultz, J. *Macromolecules* **1998**, *31*, 2545.
- (32) Špeváček, J.; Schneider, B. *Adv. Colloid. Interface Sci.* **1987**, *27*, 81.
- (33) Lotz, B.; Kovacs, A. J. *ACS Polym. Prepr.* **1969**, *10*, 820.
- (34) Loo, Y. L.; Register, R. A.; Ryan, A. J. *Phys. Rev. Lett.* **2000**, *84*, 4120.
- (35) Zhang, J.; Duan, Y.; Sato, H.; Shen, D.; Yan, S.; Noda, I.; Ozaki, Y. *J. Phys. Chem. B* **2005**, *109*, 5586.
- (36) Blundell, D. J.; MacKerron, D. H.; Fuller, W.; Mahendrasingam, A.; Martin, C.; Oldman, R. J.; Rule, R. J.; Riekel, C. *Polymer* **1996**, *37*, 3303.
- (37) Nielsen, J. R.; Woollett, A. H. *J. Chem. Phys.* **1957**, *26*, 1391.
- (38) Yan, S.; Petermann, J. *Yang D. J. Polym. Sci., Polym. Phys. Ed.* **1997**, *35*, 1415.
- (39) Yan, S.; Katzenberg, F.; Petermann, J. *J. Polym. Sci., Polym. Phys. Ed.* **1999**, *37*, 1893.
- (40) Yang, D. C.; Thomas, E. L. *J. Mater. Sci.* **1984**, *19*, 2098.
- (41) Könnecke, K.; Rebage, G. *Colloid Polym. Sci.* **1981**, *259*, 1062.
- (42) Bunn, C. W. *Trans. Faraday Soc.* **1939**, *35*, 482.
- (43) Wittmann, J. C.; Lotz, B. *Prog. Polym. Sci.* **1990**, *15*, 909.